# Studying cavitation with Basilisk

Mandeep SAINI*, Xiangbin CHEN, Stephane ZALESKI, Daniel FUSTER

Basilisk and Gerris users meeting

Paris 2023

# Motivations to study cavitation

1nm — $1\mu$m — 1mm — 1m → Bubble size

| Nano Bubbles | Biomedical application | Industrial & Engineering | Naval & Defense |
|---|---|---|---|
| a) Waste water treatment | a) HIFU therapy | a)Surface treatment and cleaning | a) Underwater explosions |
| b) Enhnced ultra-sound contrast and drug delivery | b) Drug delivery | b) Turbines and hydraulic pumps | b) Seismic airguns |
| | c) Histotripsy | c) Sono-chemistry | c) Super cavitation |

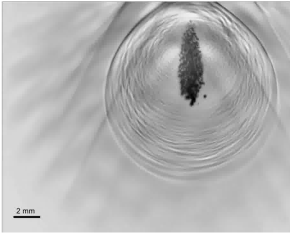


Shockwave histotripsy
Courtesy:S.W. Choi(youtube)

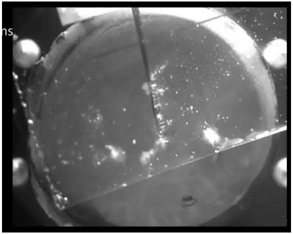

Surface cleaning
Courtesy:BuBclean(youtube)

Underwater explosion
Courtesy:Atomic test channel(youtube)

# Tool

We use two phase all-Mach solver of basilisk.

http://basilisk.fr/sandbox/fuster/Allmach3.0/two-phase-compressible.h

Journal of Computational Physics 374 (2018) 752–768

ELSEVIER

Contents lists available at ScienceDirect

Journal of Computational Physics

www.elsevier.com/locate/jcp

## An all-Mach method for the simulation of bubble dynamics problems in the presence of surface tension

Daniel Fuster *, Stéphane Popinet

*Sorbonne Université, Centre National de la Recherche Scientifique, UMR 7190, Institut Jean Le Rond D'Alembert, F-75005 Paris, France*

A R T I C L E   I N F O

*Article history:*
Received 26 March 2018
Received in revised form 20 July 2018
Accepted 29 July 2018
Available online 9 August 2018

*Keywords:*
All-Mach formulation
Bubble dynamics
Multiphase flows
Compressible flows
Volume-of-fluid method

A B S T R A C T

This paper presents a generalization of an all-Mach formulation for multiphase flows accounting for surface tension and viscous forces. The proposed numerical method is based on the consistent advection of conservative quantities and the advection of the color function used in the Volume of Fluid method avoiding any numerical diffusion of mass, momentum and energy across the interface during the advection step. The influence of surface tension and liquid compressibility on the dynamic response of the bubbles is discussed by comparing the full 3D solution with the predictions provided by the Rayleigh–Plesset equation for two relevant problems related to the dynamic response of bubbles to pressure disturbances: The linear oscillation of a single bubble in an acoustic field and the Rayleigh collapse problem. Finally, the problem of the collapse of a bubble close to a wall is compared with experimental results showing the robustness of the method to simulate the collapse of air bubbles in liquids in problems where bubbles generate a high velocity liquid jet.

# Overview of my PhD

1. We understand heterogeneous bubble nucleation and dynamics of microlayer formation using Basilisk.

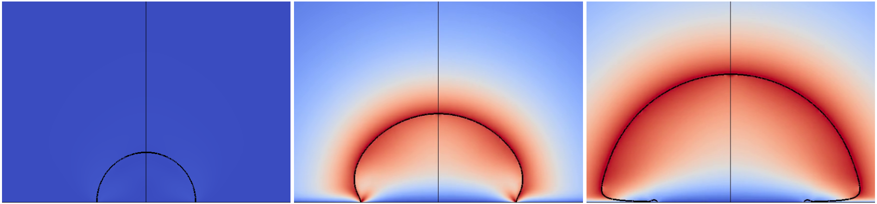

Stable bubble

Unstable bubble
No microlayer

Unstable bubble
microlayer

# Overview of my PhD

1. We understand heterogeneous bubble nucleation and dynamics of microlayer formation using Basilisk.

2. We understand the jetting during the collapse of bubble attached to wall.

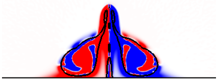

Jet parallel to wall

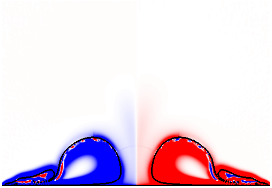

Jet normal to wall

# Overview of my PhD

1. We understand heterogeneous bubble nucleation and dynamics of microlayer formation using Basilisk.

2. We understand the jetting during the collapse of bubble attached to wall.

3. We also improve the understanding multi-bubble cavitation.
(Secondment at POF Utwente)

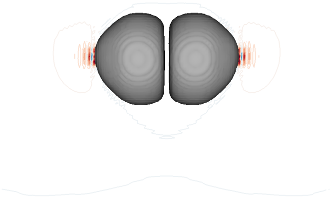

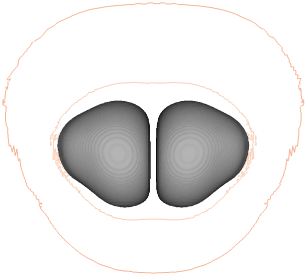

# Overview of my PhD

1. We understand heterogeneous bubble nucleation and dynamics of microlayer formation using Basilisk.

2. We understand the jetting during the collapse of bubble attached to wall.

3. We also improve the understanding multi-bubble cavitation.
(Secondment at POF Utwente)

# Nucleation threshold (Quasi-static theory)

$$p_L < \text{critical(p)}$$

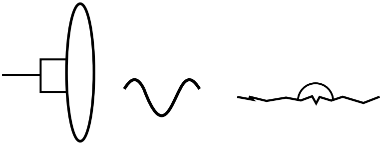


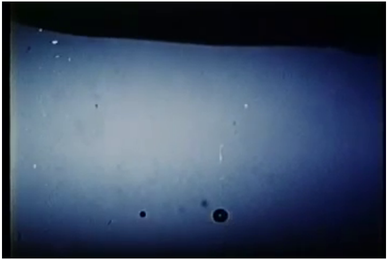

Courtesy:NCFM

# Nucleation threshold (Quasi-static theory)

$p_L <$ critical(p)

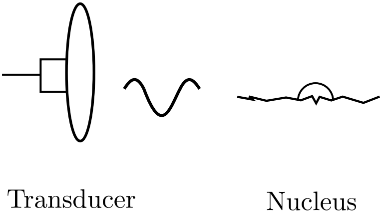


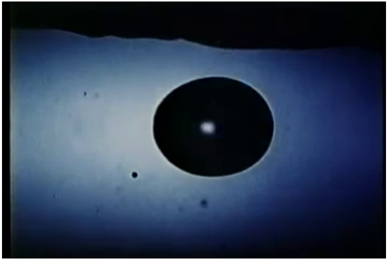

Courtesy:NCFM

# Nucleation threshold (Quasi-static theory)

$p_L < \text{critical(p)}$

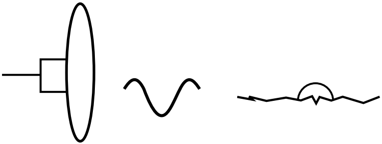

Transducer Nucleus

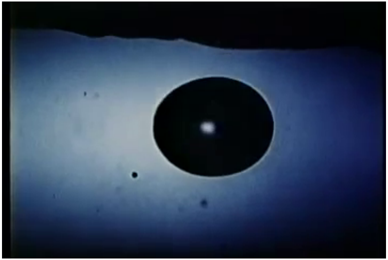

Courtesy:NCFM

$p_{L,0} \to p_L$

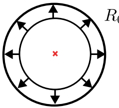


$\boxed{\text{Blake's threshold and radius}}$

$$\frac{R_{cr}}{R_0} = \left(\frac{3}{2}\gamma\frac{R_0 p_{L,0}}{\sigma}\left(1+2\frac{\sigma}{R_0 p_{L,0}}\right)\right)^{3\gamma-1} = g\left(\frac{\sigma}{R_0 p_{L,0}}\right)$$

$$\frac{p_{cr}}{p_{L,0}} = -\left(\frac{3}{2}\gamma\frac{R_0 p_{L,0}}{\sigma}\left(1+2\frac{\sigma}{R_0 p_{L,0}}\right)\right)^{\frac{1}{1-3\gamma}} 2\frac{\sigma}{R_0 p_{L,0}}\left(1-\frac{1}{3\gamma}\right) = f\left(\frac{\sigma}{R_0 p_{L,0}}\right)$$

# Numerical predictions

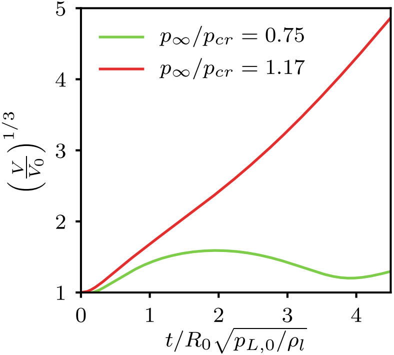


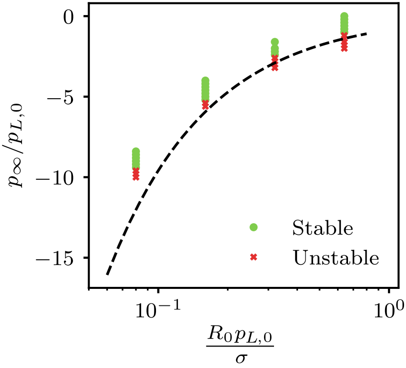


$$\frac{p_{cr}}{p_{L,0}} = f\left(\frac{\sigma}{R_0 p_{L,0}}\right)$$

# Bubbles attached to walls (quasi-static theory)

$p_{L,0} \to p_L$

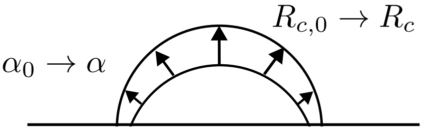

# Bubbles attached to walls (quasi-static theory)

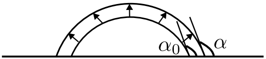


$\alpha = \alpha_0$

Free slip

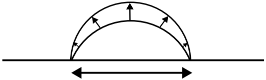

$c = c_0$

Pinning

# Bubbles attached to walls (quasi-static theory)

Air-Water

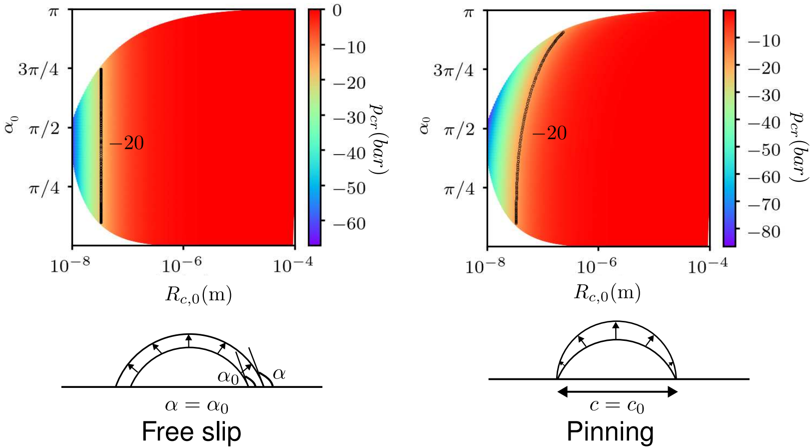

# Effect of boundary condition

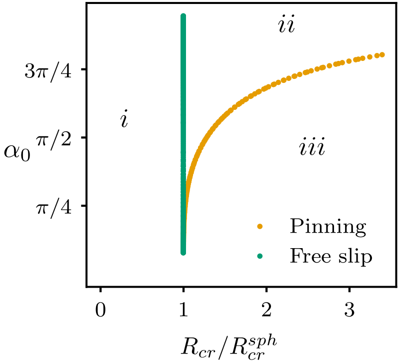

# Effect of boundary condition

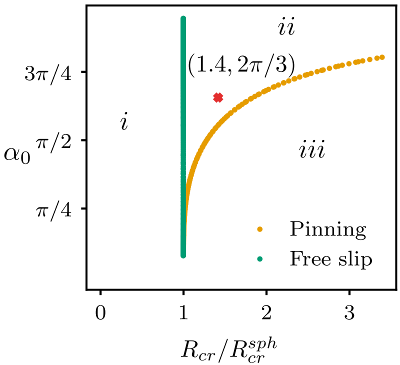


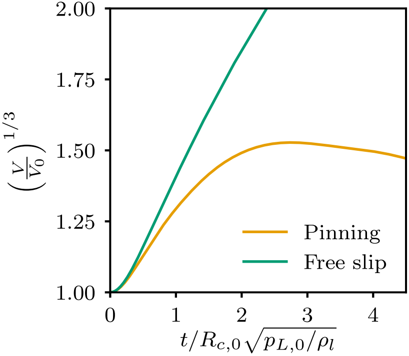


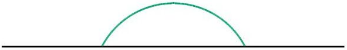

Free slip

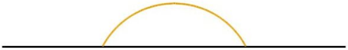

Pinning

# Effect of boundary condition

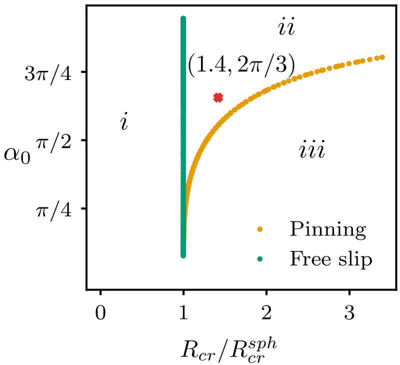


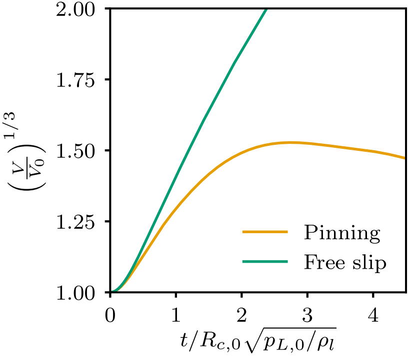


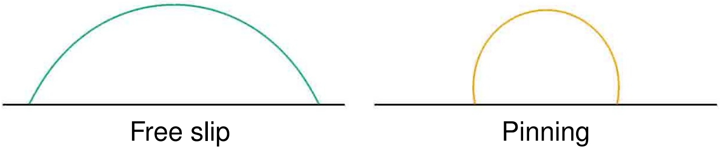

# Effect of boundary condition

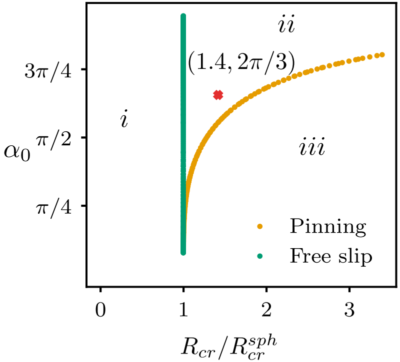


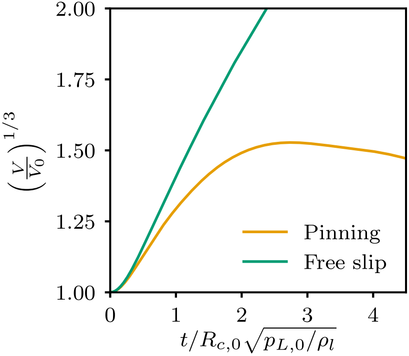


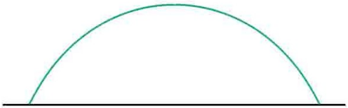

Free slip

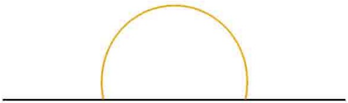

Pinning

Pinning of contact line acts as a secondary effect that stabilizes the nuclei.
Pinning effects become increasingly important as $\alpha_0$ increases.

# Complete dynamics using a contact line model

# Contact line model

Standard no-slip boundary condition predicts logarithmically diverging shear stresses.

# Contact line model

Standard no-slip boundary condition predicts logarithmically diverging shear stresses.

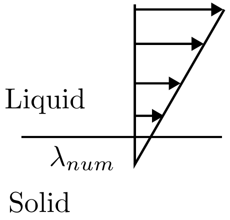


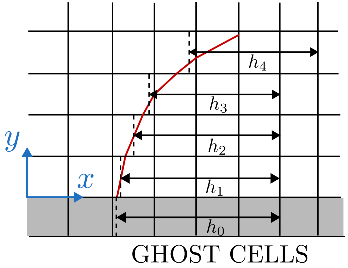


$$u_x = \lambda_{num} \frac{\partial u_x}{\partial y}$$

$$\frac{\partial h}{\partial x} = -\tan(\alpha)$$

$\alpha$ - static contact angle (imposed at smallest grid)


Afkhami, Shahriar, et al. "Transition in a numerical model of contact line dynamics and forced dewetting." Journal of Computational Physics (2018).
Kamal, Catherine, et al. "Dynamic drying transition via free-surface cusps." Journal of fluid mechanics (2019)

# Problem setup (Axisymmetric)

Far away $p_{L,0} \to p_{L,0} - \Delta p$

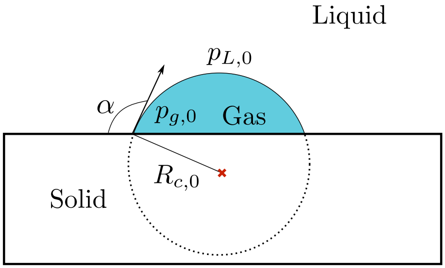

# Problem setup (Axisymmetric)

Far away $p_{L,0} \to p_{L,0} - \Delta p$

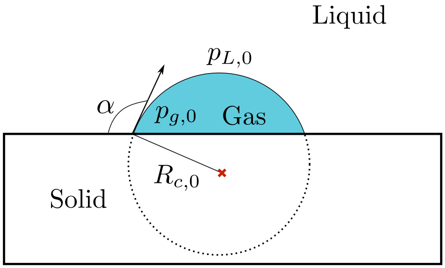


$$\text{Bubble shape}(t) = \mathcal{F}(\Delta p, p_{L,0}, \rho_l, \rho_g, \mu_l, \mu_g, \sigma, R_{c,0}, \alpha, c_l)$$

# Problem setup (Axisymmetric)

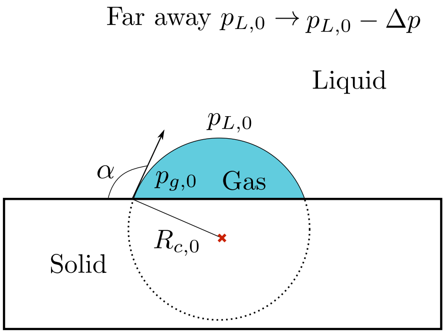


Bubble shape $\left(t^* = \frac{tU_c}{R_{c,0}}\right) = \mathcal{G}\left(p^*, \rho^*, m, \mathrm{Oh}, \mathrm{Ca}, \mathrm{Ma}, \alpha\right)$

$$p* = \frac{\Delta p}{p_{L,0}}, \qquad \rho^* = \frac{\rho_g}{\rho_l}, \qquad m = \frac{\mu_g}{\mu_l}$$

$$\mathrm{Oh} = \frac{\mu_l}{\rho_l \sigma R_{c,0}}, \qquad \mathrm{Ca} = \frac{\mu_l U_c}{\sigma}, \qquad \mathrm{Ma} = \frac{U_c}{c_l}, \qquad \alpha$$

Characteristic scales: $U_c = \sqrt{\frac{2}{3}\frac{\Delta p}{\rho_l}}$, $L_c = R_{c,0}$, $\rho_c = \rho_l$

# Problem setup (Axisymmetric)

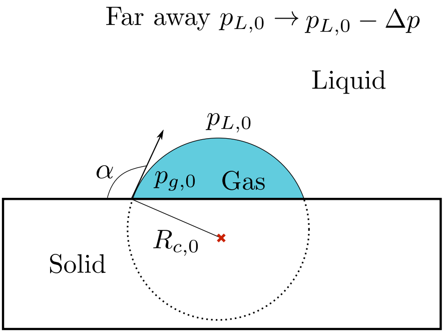


$$\text{Bubble shape}\left(t^* = \frac{tU_c}{R_{c,0}}\right) = \mathcal{G}\left(p^*, \rho^*, m, \mathrm{Oh}, \mathrm{Ca}, \mathrm{Ma}, \alpha\right)$$

$$p* = \frac{\Delta p}{p_{L,0}}, \qquad \rho^* = \frac{\rho_g}{\rho_l}, \qquad m = \frac{\mu_g}{\mu_l}$$

$$\mathrm{Oh} = \frac{\mu_l}{\rho_l \sigma R_{c,0}}, \qquad \mathrm{Ca} = \frac{\mu_l U_c}{\sigma}, \qquad \mathrm{Ma} = \frac{U_c}{c_l}, \qquad \alpha$$

Characteristic scales: $U_c = \sqrt{\frac{2}{3}\frac{\Delta p}{\rho_l}}$, $L_c = R_{c,0}$, $\rho_c = \rho_l$

# Problem setup (Axisymmetric)

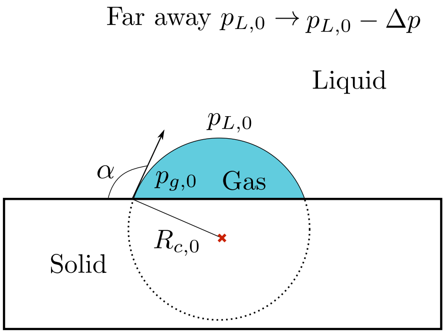


$$\text{Bubble shape}\left(t^* = \frac{tU_c}{R_{c,0}}\right) = \mathcal{G}\left(p^*, \rho^*, m, \mathrm{Oh}, \mathrm{Ca}, \mathrm{Ma}, \alpha\right)$$

To simplify, we fix $\rho^* = 10^{-3},\ m = 10^{-2},\ \mathrm{Ma} = 0.003 (U_c \ll c_l)$

$$\text{Bubble shape}(t^*) = \mathcal{G}\left(p^*, \mathrm{Oh}, \mathrm{Ca}, \alpha\right)$$

# Problem setup (Axisymmetric)

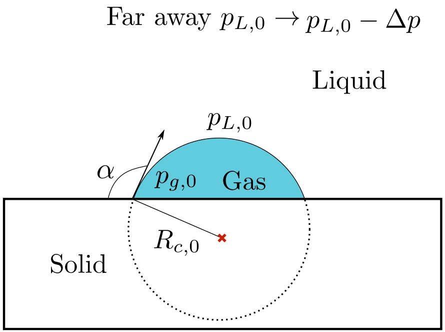


$$\text{Bubble shape}\left(t^* = \frac{tU_c}{R_{c,0}}\right) = \mathcal{G}\left(p^*, \rho^*, m, \mathrm{Oh}, \mathrm{Ca}, \mathrm{Ma}, \alpha\right)$$

To simplify, we fix $\rho^* = 10^{-3},\ m = 10^{-2},\ \mathrm{Ma} = 0.003 (U_c \ll c_l)$

$$\text{Bubble shape}(t^*) = \mathcal{G}\left(p^*, \mathrm{Oh}, \mathrm{Ca}, \alpha\right)$$

Alternatively, we can use $\mathrm{Re} = \frac{\mathrm{Ca}}{\mathrm{Oh}^2}$ and $\mathrm{We} = \frac{\mathrm{Ca}^2}{\mathrm{Oh}^2}$

# Overall view

$$\mathrm{Ca}_{cr}(\Delta p = \Delta p_{cr}) = \mathrm{Oh}\sqrt{2\left(1-\frac{1}{3\gamma}\right)\left[\frac{3}{2}\left(\frac{\mathrm{Ca}_0}{\mathrm{Oh}}\right)^2\gamma\left(1+2\left(\frac{\mathrm{Oh}}{\mathrm{Ca}_0}\right)^2\right)\right]^{1/(1-3\gamma)}}$$

($\alpha = 90^\circ$, Free slip)

$\mathrm{Ca} \propto \sqrt{\Delta p}$ and $\mathrm{Oh} \propto \frac{1}{\sqrt{R_{c,0}}}$

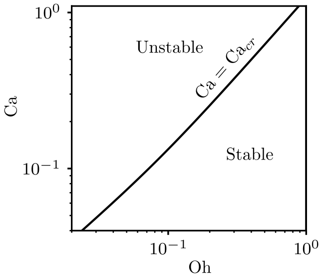

# Overall view

$$\mathrm{Ca}_{cr}(\Delta p = \Delta p_{cr}) = \mathrm{Oh}\sqrt{2\left(1-\frac{1}{3\gamma}\right)\left[\frac{3}{2}\left(\frac{\mathrm{Ca}_0}{\mathrm{Oh}}\right)^2\gamma\left(1+2\left(\frac{\mathrm{Oh}}{\mathrm{Ca}_0}\right)^2\right)\right]^{1/(1-3\gamma)}}$$

($\alpha = 90°$, Free slip)

$\mathrm{Ca} \propto \sqrt{\Delta p}$ and $\mathrm{Oh} \propto \frac{1}{\sqrt{R_{c,0}}}$

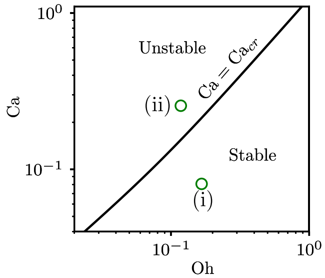


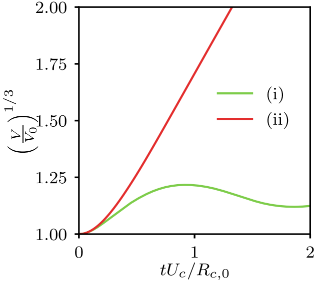


(i)

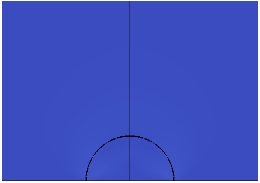

(ii)

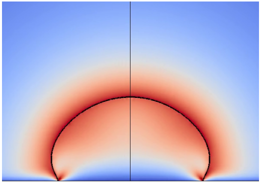

Atchley, Anthony A., and Andrea Prosperetti. "The crevice model of bubble nucleation." The Journal of the Acoustical Society of America 86.3 (1989)

# Overall view

$$\mathrm{Ca}_{cr}(\Delta p = \Delta p_{cr}) = \mathrm{Oh}\sqrt{2\left(1-\frac{1}{3\gamma}\right)\left[\frac{3}{2}\left(\frac{\mathrm{Ca}_0}{\mathrm{Oh}}\right)^2\gamma\left(1+2\left(\frac{\mathrm{Oh}}{\mathrm{Ca}_0}\right)^2\right)\right]^{1/(1-3\gamma)}}$$

($\alpha = 90°$, Free slip)

$\mathrm{Ca} \propto \sqrt{\Delta p}$ and $\mathrm{Oh} \propto \frac{1}{\sqrt{R_{c,0}}}$

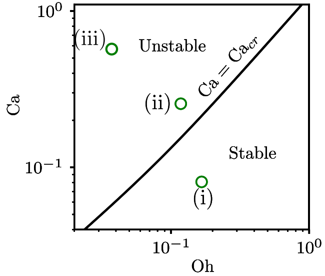


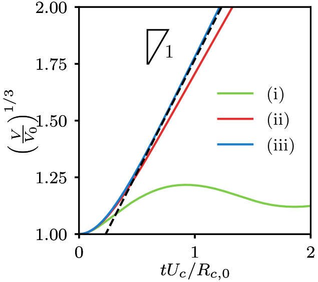


(i)

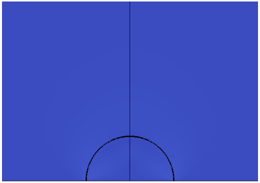

(ii)

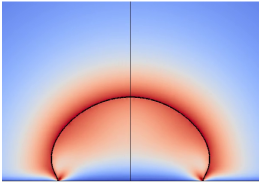

(iii)

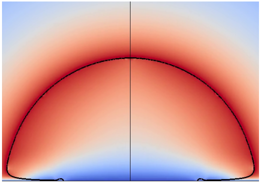

Atchley, Anthony A., and Andrea Prosperetti. "The crevice model of bubble nucleation." The Journal of the Acoustical Society of America 86.3 (1989)

# Overall view

$$\mathrm{Ca}_{cr}(\Delta p = \Delta p_{cr}) = \mathrm{Oh}\sqrt{2\left(1-\frac{1}{3\gamma}\right)\left[\frac{3}{2}\left(\frac{\mathrm{Ca}_0}{\mathrm{Oh}}\right)^2\gamma\left(1+2\left(\frac{\mathrm{Oh}}{\mathrm{Ca}_0}\right)^2\right)\right]^{1/(1-3\gamma)}}$$

($\alpha = 90^\circ$, Free slip)

$\mathrm{Ca} \propto \sqrt{\Delta p}$ and $\mathrm{Oh} \propto \frac{1}{\sqrt{R_{c,0}}}$

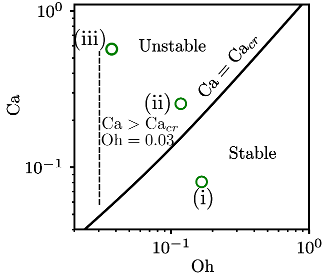


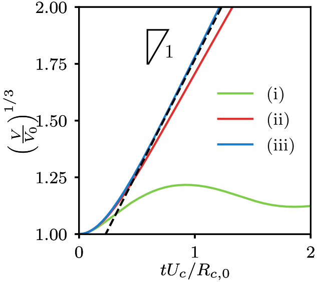


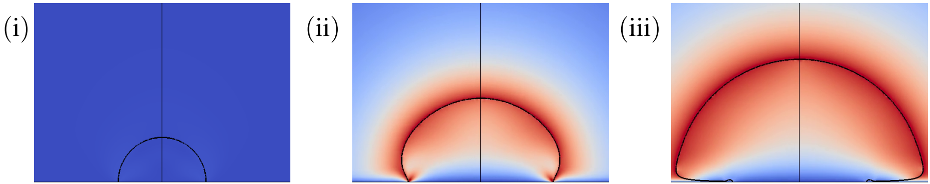


Atchley, Anthony A., and Andrea Prosperetti. "The crevice model of bubble nucleation." The Journal of the Acoustical Society of America 86.3 (1989)

# Characteristic points on bubble interface

Three characteristic velocities: (a) Bubble height $u_h$

(b) Contact line $u_{CL}$

(c) Bubble width $u_{c_m}$

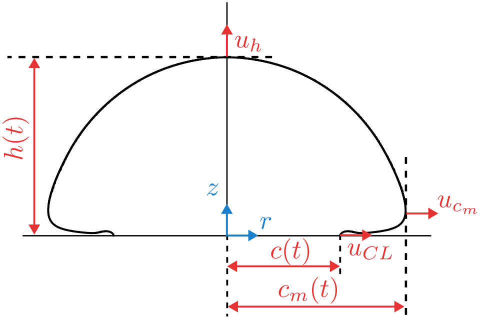

# Effect of capillary number

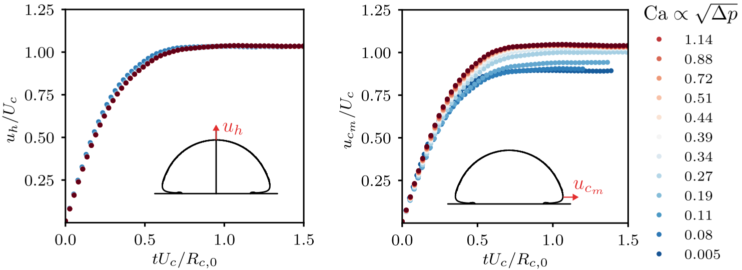


Fixed parameters

$$\mathrm{Oh} \propto \frac{1}{\sqrt{R_{c,0}}} = 0.032$$

$$\frac{\lambda_{num}}{R_{c,0}} = 0.01$$

$$U_c = \sqrt{\frac{2}{3}\frac{\Delta p}{\rho_l}}$$

# Effect of capillary number

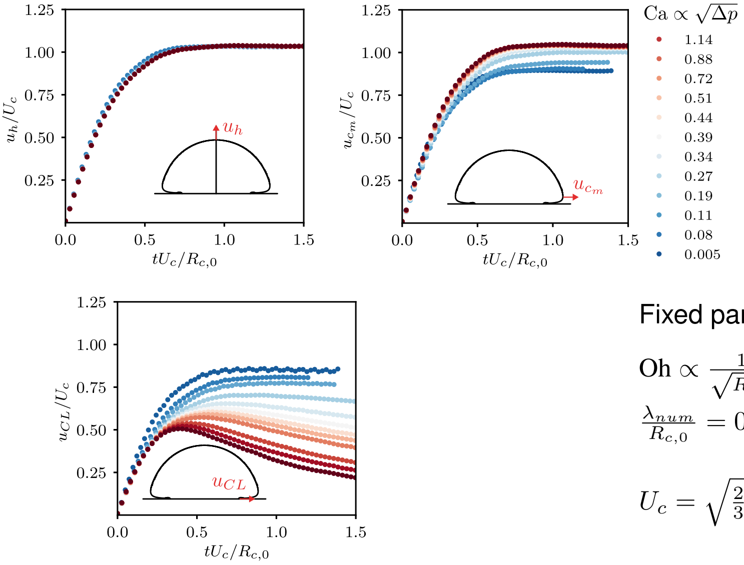


## Fixed parameters

$$\mathrm{Oh} \propto \frac{1}{\sqrt{R_{c,0}}} = 0.032$$

$$\frac{\lambda_{num}}{R_{c,0}} = 0.01$$

$$U_c = \sqrt{\frac{2}{3}\frac{\Delta p}{\rho_l}}$$

# Effect of capillary number

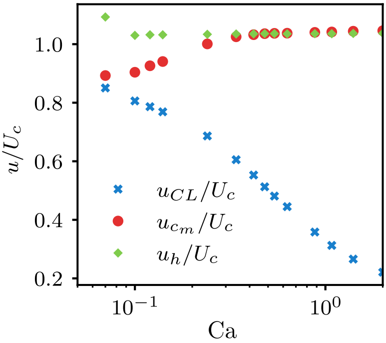


$\mathrm{Oh} = 0.032$

$\frac{\lambda_{num}}{R_{c,0}} = 0.01$

varying $\mathrm{Ca} = \frac{\mu U_c}{\sigma}$

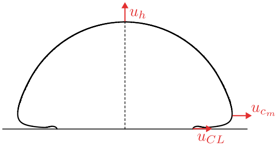


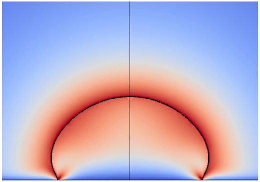

Small Ca

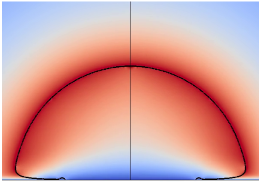

Large Ca

# Can we say more about the contact line velocity?

$$\mathrm{Ca}(u_{CL}) = \frac{U_{CL}}{\sigma/\mu}$$

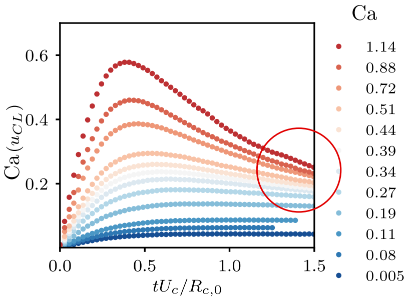


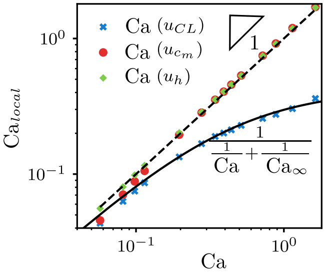

# Effect of contact angle

$\mathrm{Oh} = 0.032 \ll 1 \ \frac{\lambda_{num}}{R_{c,0}} = 0.01$

varying $\mathrm{Ca} = \frac{\mu U_c}{\sigma}$ and $\alpha$

$$\mathrm{Ca}(u_{CL}) = \frac{1}{\frac{1}{\mathrm{Ca}} + \frac{1}{\mathrm{Ca}_\infty}}$$

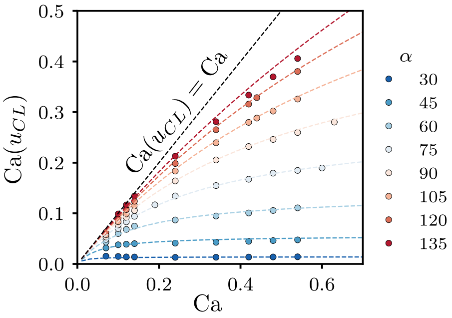

# Effect of contact angle

$\mathrm{Oh} = 0.032 \ll 1$ $\frac{\lambda_{num}}{R_{c,0}} = 0.01$

varying $\mathrm{Ca} = \frac{\mu U_c}{\sigma}$ and $\alpha$

$$\mathrm{Ca}(u_{CL}) = \frac{1}{\frac{1}{\mathrm{Ca}} + \frac{1}{\mathrm{Ca}_\infty}}$$

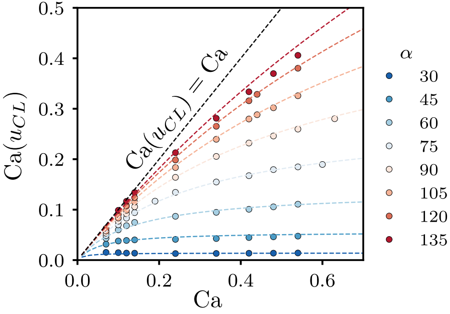


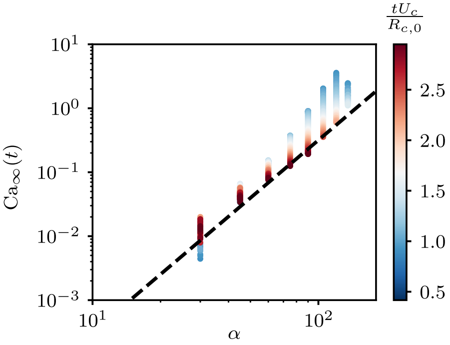

# Effect of contact angle

$\mathrm{Oh} = 0.032 \ll 1 \quad \frac{\lambda_{num}}{R_{c,0}} = 0.01$

varying $\mathrm{Ca} = \frac{\mu U_c}{\sigma}$ and $\alpha$

$$\mathrm{Ca}(u_{CL}) = \frac{1}{\frac{1}{\mathrm{Ca}} + \frac{1}{\mathrm{Ca}_\infty}}$$

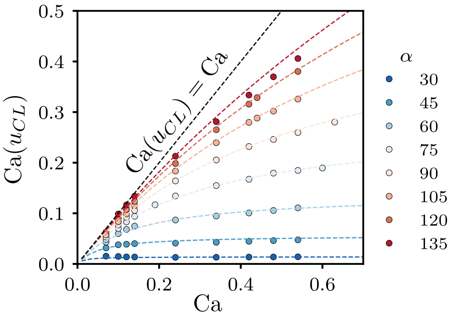


Recall Cox-Voinov law

$$\cancel{\alpha_{app}}^{\,0} = \alpha^3 + 9\mathrm{Ca}(u_{CL}) ln(L/\lambda)$$

$$\mathrm{Ca}(u_{CL}) = \frac{1}{9 ln(\lambda/L)}\alpha^3$$

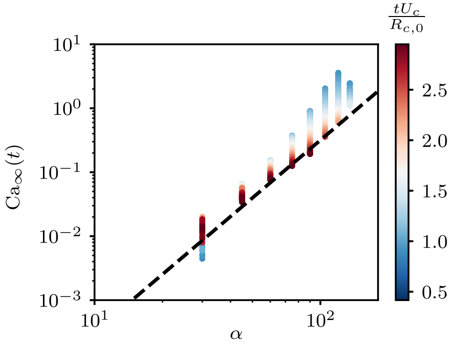

# Effect of contact angle

$\mathrm{Oh} = 0.032 \ll 1 \quad \frac{\lambda_{num}}{R_{c,0}} = 0.01$

varying $\mathrm{Ca} = \frac{\mu U_c}{\sigma}$ and $\alpha$

$$\mathrm{Ca}(u_{CL}) = \frac{1}{\frac{1}{\mathrm{Ca}} + \frac{1}{\mathrm{Ca}_\infty}}$$

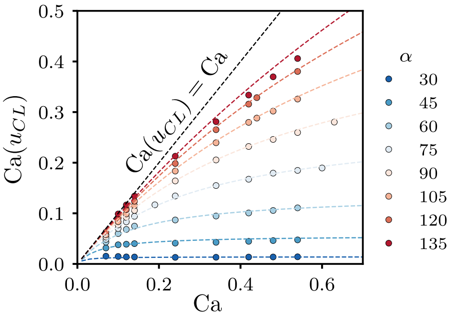


$\mathrm{Ca}_\infty$ varies with cube of $\alpha$

Recall Cox-Voinov law

$$\cancel{\alpha_{app}}^{\,0} = \alpha^3 + 9\mathrm{Ca}(u_{CL}) ln(L/\lambda)$$

$$\mathrm{Ca}(u_{CL}) = \frac{1}{9 ln(\lambda/L)} \alpha^3$$

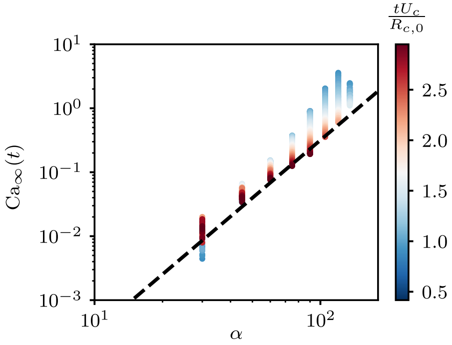

# Overall dynamics

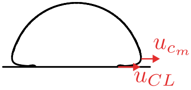


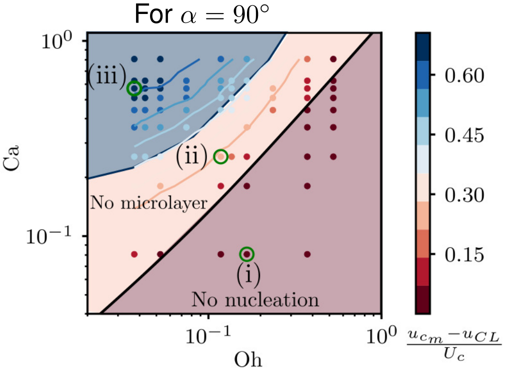


(i)

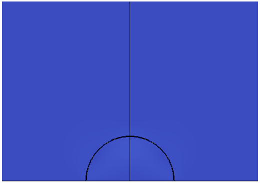

(ii)

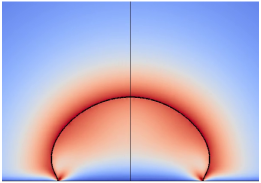

(iii)

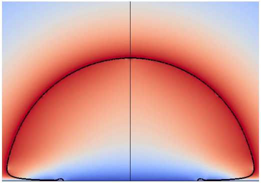

# Overall dynamics

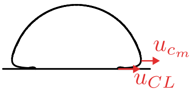


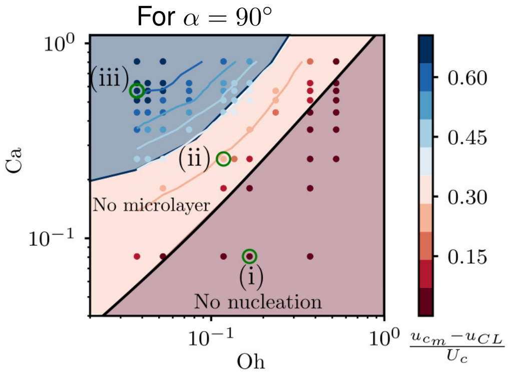


Microlayer starts to form when $\mathrm{Ca} \ll \mathrm{Ca}_{cr}$ and for Ohnesorge number given by bubble size.

# Overall dynamics

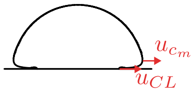


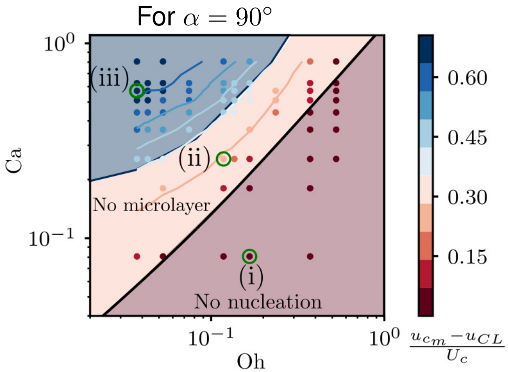


Microlayer starts to form when $\mathrm{Ca} \ll \mathrm{Ca}_{cr}$ and for Ohnesorge number given by bubble size.

# Overall dynamics

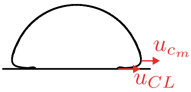


For $\alpha = 90°$

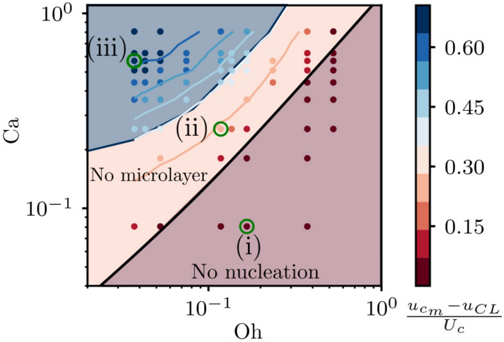


Microlayer starts to form when $\mathrm{Ca} \ll \mathrm{Ca}_{cr}$ and for Ohnesorge number given by bubble size.

Also, $\mathrm{Re} = \frac{\mathrm{Ca}}{\mathrm{Oh}^2} \to \infty$ and $\mathrm{We} = \frac{\mathrm{Ca}^2}{\mathrm{Oh}^2} \to \infty$.

Implying that inertial effects can be important at microlayer scale.

# Structure of microlayer

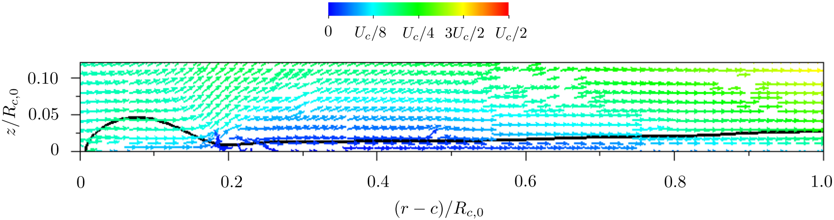


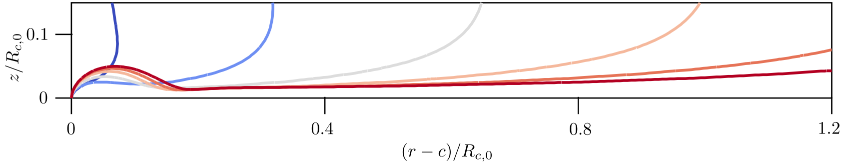

# Scaling for the height of microlayer

h(Bretherton)

$$\left(\frac{\mu}{\sigma}U_c\right)^{2/3} a$$

h(Boundary layer)

$$\left(\frac{\mu}{\rho_l}\frac{x}{U_c}\right)^{1/2}$$

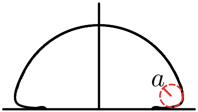

# Scaling for the height of microlayer

$$\text{h(Bretherton)} \quad \sim \quad \text{h(Boundary layer)}$$

$$\left(\frac{\mu}{\sigma}U_c\right)^{2/3} a \quad \sim \quad \left(\frac{\mu}{\rho_l}\frac{x}{U_c}\right)^{1/2}$$

$$\frac{x}{R_{c,0}} \sim \left(\frac{a}{R_{c,0}}\right)^2 \mathrm{Ca}^{1/3}\mathrm{We} \sim \mathcal{H}(a, \mathrm{Ca}, \mathrm{We})$$

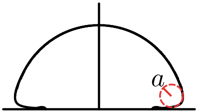

# Scaling for the height of microlayer

h(Bretherton) $\sim$ h(Boundary layer)

$$\left(\frac{\mu}{\sigma}U_c\right)^{2/3} a \sim \left(\frac{\mu}{\rho_l}\frac{x}{U_c}\right)^{1/2}$$

$$\frac{x}{R_{c,0}} \sim \left(\frac{a}{R_{c,0}}\right)^2 \mathrm{Ca}^{1/3}\mathrm{We} \sim \mathcal{H}(a, \mathrm{Ca}, \mathrm{We})$$

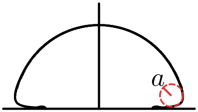


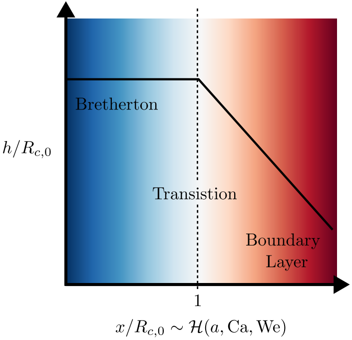


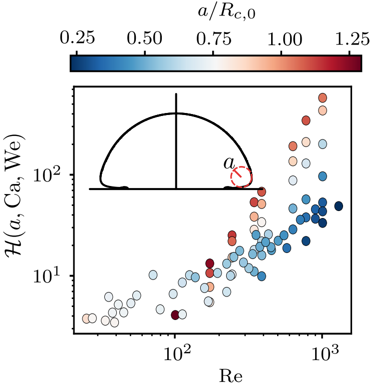

# Scaling for the height of microlayer

$$\text{h(Bretherton)} \sim \text{h(Boundary layer)}$$

$$\left(\frac{\mu}{\sigma}U_c\right)^{2/3} a \sim \left(\frac{\mu}{\rho_l}\frac{x}{U_c}\right)^{1/2}$$

$$\frac{x}{R_{c,0}} \sim \left(\frac{a}{R_{c,0}}\right)^2 \mathrm{Ca}^{1/3}\mathrm{We} \sim \mathcal{H}(a, \mathrm{Ca}, \mathrm{We})$$

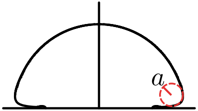


BL theory works for large $\mathcal{H}$ but it misses effect of surface tension

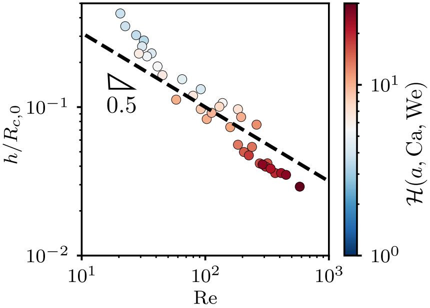


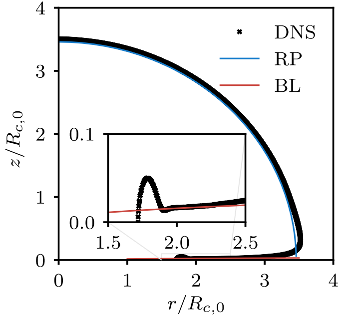

# Effect of contact angle

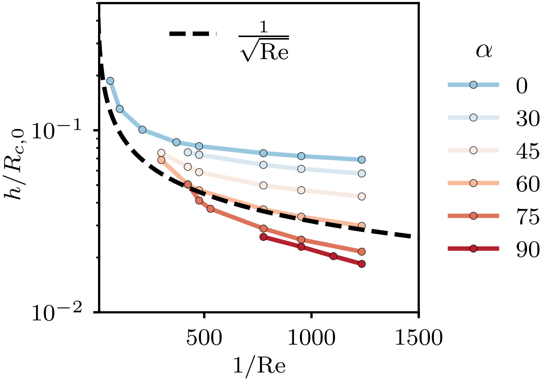

# Conclusions

- Resolved simulations of microlayer formation are performed using slip model.
- Our results show that microlayer forms in the regimes where $\mathrm{Ca} \sim \mathrm{Ca}_{cr}$ for given $\mathrm{Oh}$.
- In this regime, the contact line capillary number takes an asymptotic velocity, thus its motion is controlled only by visco-capillary effects, inertial effects can also play important role at scale of microlayer height.
- In this limiting regime, we can approximately predict the structure of microlayer from boundary layer approximation, while neglecting the surface tension effects.

# THANK YOU

http://basilisk.fr/sandbox/msaini